HHS Public Access

Author manuscript

J Bone Miner Res. Author manuscript; available in PMC 2023 April 01.

Published in final edited form as:

J Bone Miner Res. 2022 April ; 37(4): 616–628. doi:10.1002/jbmr.4495.

Short Cyclic Regimen with Parathyroid Hormone (PTH) Results in Prolonged Anabolic Effect Relative to Continuous Treatment Followed by Discontinuation in Ovariectomized Rats

Wei-Ju Tseng[1], **Wonsae Lee**[1], **Hongbo Zhao**[1], **Yang Liu**[1,2], **Wenzheng Wang**[1,3], **Chantal M. J. de Bakker**[1,4], **Yihan Li**[1], **Carlos Osuna**[1], **Wei Tong**[1,3], **Luqiang Wang**[1,5], **Xiaoyuan Ma**[1,6], **Ling Qin**[1], **X. Sherry Liu**[1,*]

[1]McKay Orthopaedic Research Laboratory, Department of Orthopaedic Surgery, Perelman School of Medicine, University of Pennsylvania, Philadelphia, PA, USA.

[2]Department of Orthodontics, Stomatological Hospital of Chongqing Medical University, Chongqing, China

[3]Department of Orthopaedics, Union Hospital, Tongji Medical College, Huazhong University of Science and Technology, Wuhan, Hubei, China

[4]Department of Radiology, Cumming School of Medicine, McCaig Institute for Bone and Joint Health, University of Calgary, Calgary, Canada.

[5]Department of Orthopaedics, National Cancer Center/National Clinical Research Center for Cancer/Cancer Hospital, Chinese Academy of Medical Sciences and Peking Union Medical College, Beijing 100021, China

[6]Department of Orthopaedics, Shandong University Qilu Hospital, Shandong University, Jinan, China

Abstract

Despite the potent effect of intermittent PTH treatment on promoting new bone formation, BMD rapidly decreases upon discontinuation of PTH administration. To uncover the mechanisms behind this adverse phenomenon, we investigated the immediate responses in bone microstructure and bone cell activities to PTH treatment withdrawal and the associated long-term consequences. Unexpectedly, intact female and estrogen-deficient female rats had distinct responses to the discontinuation of PTH treatment. Significant tibial bone loss and bone microarchitecture deterioration occurred in estrogen-deficient rats, with the treatment benefits of PTH completely lost 9 weeks after discontinuation. In contrast, no adverse effect was observed in intact rats, with sustained treatment benefit 9 weeks after discontinuation. Intriguingly, there is an extended anabolic period during the first week of treatment withdrawal in estrogen-deficient rats, during which no significant change occurred in the number of osteoclasts while the number of osteoblasts remained elevated compared to vehicle-treated rats. However, increases in number of osteoclasts and decreases in number of osteoblasts occurred 2 weeks after discontinuation of PTH treatment,

*To whom correspondence should be addressed: X. Sherry Liu, McKay Orthopaedic Research Laboratory, Department of Orthopaedic Surgery, University of Pennsylvania, 371 Stemmler Hall, 36th Street and Hamilton Walk, Philadelphia, PA 19104, USA, xiaoweil@pennmedicine.upenn.edu, Phone: 1-215-746-4668.

leading to significant reduction in bone mass and bone microarchitecture. To leverage the extended anabolic period upon early withdrawal from PTH, a cyclic administration regimen with repeated cycles of on and off PTH treatment was explored. We demonstrated that the cyclic treatment regimen efficiently alleviated the PTH withdrawal-induced bone loss, improved bone mass, bone microarchitecture, and whole-bone mechanical properties, and extended the treatment duration.

Keywords

Parathyroid hormone; PTH treatment discontinuation; bone microarchitecture; bone mechanics; bone cell activities; cyclic treatment regimen

1. Introduction:

Osteoporosis is a disease characterized by significant reductions in overall bone density and structural integrity, causing skeletal fragility and an increased risk of bone fractures [1]. Risks of osteoporosis and fragility fracture significantly increase in women post menopause, as rapid decline in estrogen levels during menopause leads to accelerated bone resorption that outpaces bone formation. Current treatments for postmenopausal osteoporosis focus on either inhibiting bone resorption using anti-resorptive agents or promoting bone formation using anabolic agents [2]. Parathyroid hormone is the first clinically approved anabolic agent for osteoporosis when administered intermittently. Its mechanism of action is to promote bone remodeling and to shift the balance of remodeling towards increased bone formation [3–5], and thereby rapidly increases bone mass and reduces the risk of fractures.

In clinical practice, the recommended duration of PTH treatment is limited to 18–24 months due to the theoretical risk of developing osteosarcoma [6–8]. However, osteoporosis in postmenopausal women and elderly men is a life-long, chronic condition. Despite the potent effect of PTH on promoting new bone formation, if not followed by an antiresorptive agent, the gains in bone mineral density (BMD) are quickly lost upon withdrawal from PTH treatment [9–11]. In a randomized, 2-year study with a 1-year treatment of PTH1–84 followed by a 1-year treatment of alendronate or placebo, women who were randomized to receive placebo after PTH treatment experienced a nearly 2% loss in BMD at the spine. Moreover, trabecular bone is more susceptible to bone loss upon PTH discontinuation, demonstrated by a striking 10% decrease in the trabecular volumetric BMD at the spine [9]. However, the mechanisms behind this adverse event are not fully understood. To maximize the efficacy of PTH, it is imperative to obtain a better understanding of the structural and cellular mechanisms behind the bone loss upon discontinuation of PTH treatment. Therefore, the first objective of this study was to uncover the structural changes and cellular responses after discontinuation of intermittent PTH administration in both intact and estrogen deficient rats. By using an *in vivo* μCT imaging technique and dynamic bone histomorphometry, we discovered that, prior to the adverse effects of treatment discontinuation, there is an extended anabolic period upon early treatment withdrawal in the estrogen-deficient rats, which was further confirmed by histological analyses of bone cells. The extended anabolic period would offer a new mechanism in support of the cyclic PTH treatment regimen to maximize the bone gain and extend treatment duration. Therefore,

the second objective was to test the efficacy of a cyclic PTH treatment regimen on rescuing PTH's withdrawal effects. We hypothesized that a cyclic PTH treatment regimen with repeated cycles of on and off daily injection of PTH would best utilize the extended anabolic period upon withdrawal, resulting in extended treatment duration and significant improvement in bone mass, bone microarchitecture, and mechanical properties.

2. Materials and Methods:

2.1 Animals and treatment plans

All experiments were approved by the University of Pennsylvania's Institutional Animal Care and Use Committee. A total of 108 female Sprague Dawley rats (Charles River Laboratories, Wilmington, MA, USA) were used in this study. All rats were housed in standard conditions in groups of three rats per cage and fed ad libitum (LabDiet 5001 Rodent Diet) with unlimited access to food. For longitudinal μCT imaging studies, rats were randomly allocated to groups to minimize variation in baseline bone volume fraction between groups before being randomly assigned to treatments. For rest of the studies, rats were grouped by weight before being randomly assigned to treatments. Experiments were performed unblinded. Intermittent PTH treatment (Human Recombinant PTH1–34, Bachem, Bubendorf, Switzerland) was administered subcutaneously 5 times per week to all animals at the dose of 40 μg/kg/day, while Vehicle treatment was administered as subcutaneous injections of saline (150 μL/day, 5 times per week).

2.2 Study design

2.2.1 PTH discontinuation in intact animals—Forty intact female rats at age 16–17 weeks were used in this study. First, a longitudinal μCT imaging study was performed for a vehicle group (V3V9, receiving saline injections for 12 weeks, n=6) and a PTH-VEH group (P3V9, receiving injections of PTH for 3 weeks followed by saline for 9 weeks, n=6) where animals received *in vivo* μCT scans every 3 weeks (Figure 1A). Second, additional μCT scans were performed for a vehicle group (V3V3, n=5) and a PTH-VEH group (P3V3, n=3, Supplemental Figure 1A) at week 0, 3, 4, 5, 6 for detecting the skeletal response immediately after treatment discontinuation. Next, 20 rats were used in a histology study to assess bone cell activities and euthanized after 3-week VEH treatment (V3, n=5), 3-week PTH treatment (P3, n=5), 3-week PTH treatment followed by 1-week VEH treatment (P3V1, n=5), and followed by 2-week VEH treatment (P3V2, n=5).

2.2.2 PTH discontinuation in ovariectomized (OVX) animals—Forty-eight rats received bilateral ovariectomy surgery at 16–17 weeks of age. The study began 4 weeks after OVX to allow for development of bone loss in the OVX rats. Similar to the intact rats, 18 OVX rats were assigned to 2 groups for a longitudinal μCT imaging study: a vehicle (OVX-V3V9, n=9) group receiving saline injections for 12 weeks and a PTH-VEH group (OVX-P3V9, n=9) receiving PTH injections for 3 weeks followed by saline for 9 weeks (Figure 2A). *In vivo* μCT scans were performed the day before OVX surgery (week −4) and at weeks 0, 3, 4, 5, 6, 8, 10, and 12 of treatment. Next, 24 rats were used to assess bone cell activities after 3-week VEH treatment (OVX-V3, n=6), 3-week PTH treatment (OVX-P3, n=6), 3-week PTH treatment followed by 1-week VEH treatment (OVX-P3V1, n=6), and

followed by 2-week VEH treatments (OVX-P3V2, n=6). An additional 6 OVX rats were used for a dynamic bone histomorphometry study to confirm and quantify bone formation during the extended anabolic period within the first week of PTH discontinuation. Each rat received a sequence of multicolor fluorochrome label injections including a subcutaneous injection of calcein (green, G, 15mg/kg), intraperitoneal injection of alizarin complexone (red, R, 30mg/kg), and intraperitoneal injection of tetracycline (yellow, Y, 30mg/kg) in the order of G-R-Y-G at days −2, 5, 12, 19 (initiation of PTH 20 μg/kg/day on day 0), followed by euthanasia at day 28 (1-week after PTH discontinuation). The bone tissue deposited between the last calcein green label and bone surface was quantified as the extended anabolic period. The injections of other labels were designed for another study.

2.2.3 Cyclic treatment regimen in OVX animals—Lastly, to test the long-term efficacy of different treatment regimens, 20 OVX rats were assigned to 3 groups: VEH (18-week saline injections, n=6), PTH-VEH (9-week PTH treatment followed by 9-week vehicle treatment, n=7), and Cyclic PTH (3-week PTH followed by 3-week vehicle treatment, repeat for 3 cycles, n=7). *In vivo* μCT scans of the proximal tibia were performed the day before OVX surgery (week −4) and at week 0, 3, 6, 9, 12, 15, and 18 of treatment. Rats were euthanized after treatment and the second lumbar vertebra and the right femur were dissected and subjected to mechanical testing.

2.3 In vivo μCT scans and trabecular bone microstructure analysis

As described in [12] and [13], rats were anesthetized (4.0/2% isoflurane), and the right leg of each rat was inserted into a custom holder to ensure minimal movement during the *in vivo* μCT scan (Scanco vivaCT40, Scanco Medical AG, Brüttisellen, Switzerland). A 4-mm region of the tibia, distal to the proximal growth plate, was scanned at 10.5 μm voxel size, 55 kVp energy, 145 μA intensity, 200 ms integration time, and 1000 projections, using a 0.5mm Al filter and a standard, manufacturer-provided beam-hardening correction algorithm, resulting in a total scan time of about 20 minutes and approximate radiation dose of 0.639 Gy per scan.

The follow-up scans were registered to the baseline scan following procedures as described in our previous publications [14, 15]. Briefly, a volume of interest (VOI) of the trabecular bone compartment in the secondary spongiosa, starting approximately 2.3 mm distal from the growth plate and consisting of 200 slices (corresponding to a 2.1 mm thick section) was chosen in the last scan. By applying 3D image registration [14], the corresponding VOIs of trabecular bone in images from the previous time points were precisely identified. Representative baseline and registered follow-up images of each treatment group are shown in Figure 1B and 2B.

Bone voxels of each registered image were segmented from the bone marrow and background using Gaussian filtering (sigma=1.2 and support=2.0) and a global threshold corresponding to 564.8 mgHA/cm^3. Bone microstructural parameters including bone volume fraction (BV/TV), trabecular thickness (Tb.Th), trabecular separation (Tb.Sp), trabecular number (Tb.N), structure model index (SMI), and connectivity density (Conn.D), were evaluated for all registered VOIs [16].

2.4 Multiplexed cryohistology and dynamic bone histomorphometry

The right tibiae of rats with fluorochrome label injections were harvested and fixed in 4% paraformaldehyde (PFA) at 4 °C for 48 hours. Samples were then transferred to a solution of 20% sucrose and 2% polyvinylpyrrolidone (PVP) for 48 hours, followed by cryoembedding in Tissue-Tek O.C.T. Compound (Sakura Finetek USA Inc, Torrance, CA) using liquid nitrogen. Eight μm-thick, mineralized coronal sections were collected using cryofilm IIC tape (Section-Lab Co. Ltd., Hiroshima, Japan). Sections were attached to glass microscope slides with 1% chitosan adhesive for 48 hours. Firmly attached sections were rehydrated in a 1x phosphate buffered saline (PBS) solution for 15 min and mounted with 50% glycerol. Dark field images and fluorescent images were obtained by Axio Scan Z1 (Zeiss, Oberkochen, Germany). Bone formation sites were identified by fluorochrome labels on the bone surface. Histomorphometric measurements were performed to quantify the additional bone formation beyond the last Calcein green label, which labeled the active and mineralizing bone formation sites right before the discontinuation of 3-week PTH treatment. A region of interest in the secondary spongiosa located 1.0 – 2.5 mm below the growth plate was analyzed for each specimen. Mineral apposition rate (MAR), mineralizing surface (MS/BS), and bone formation rate over bone surface (BFR/BS) of the additional bone formation during the extended anabolic period (1 week upon discontinuation) were calculated by OsteoMeasure™ (OsteoMetrics, Atlanta, GA) according to recommendation from the ASBMR Histomorphometry Nomenclature Committee [17]. Additionally, the percent of MS/BS at the end of 3-week PTH treatment (week 3) that continued forming new bone during the extended anabolic period was also calculated.

2.5 Static Bone Histomorphometry

The right tibiae in the V3, P3, P3V1, and P3V2 group of intact and OVX rats were harvested immediately after euthanasia for methylmethacrylate (MMA) embedding. Five-μm-thick coronal sections were cut using a Polycut-S motorized microtome (Reichert, Heidelberg, Germany) for static bone histomorphometry measurements. Goldner's trichrome staining was performed to identify osteoblasts, osteoclasts, and bone surface. Furthermore, the left tibiae of OVX rats were harvested and prepared for paraffin embedding. Hematoxylin and eosin (H&E) staining was performed on five-μm-thick coronal paraffin sections to identify adipocytes and bone marrow area. All histomorphometric measurements were performed in an area 1.5–4.0 mm distal to the growth plate using Bioquant Osteo Software (Bioquant Image Analysis, Nashville, TN) and the following parameters were derived: osteoblast and osteoclast number per bone surface (N.Ob/BS and N.Oc/BS, 1/mm), the percentage of osteoblast and osteoclast surface (Ob.S/BS and Oc.S/BS, %), and adipocyte number per bone marrow area (N.Adi/Ma.Ar, 1/mm^2) [17, 18]. Blood in these rats was collected via cardiac puncture at the time of euthanasia and left at room temperature for 30 min before being placed on ice and centrifuged at 2000×g for 10 min to separate sera. Serum tartrate-resistant acid phosphatase 5b (TRAP) levels were determined by the RatTRAP™ (TRAcP 5b) ELISA immunoassay (Immunodiagnostic Systems, Scottsdale, AZ).

2.6 Ex vivo μCT Scans and Uniaxial Compression Tests for the Lumbar Vertebra L2

The second lumbar vertebrae (L2) of the cyclic treatment groups were harvested and scanned by μCT (vivaCT40, Scanco Medical AG, Brüttisellen, Switzerland) at 10.5 μm isotropic resolution. A 2.1 mm-thick trabecular VOI, which occupied the center 1/2 of the region between endplates, was identified and subjected to analysis as described previously [19]. Subsequently, the vertebral body was cut at both ends of the growth plate using a low speed diamond saw (IsoMet, Buehler, Lake Bluff, IL) with water irrigation. A ~4-mm specimen with two paralleled endplates was then obtained for the uniaxial compression test as described in [19]. The load-displacement curve generated from mechanical testing was used to calculate stiffness, peak load, and energy to failure. These mechanical properties at whole bone level were then normalized by vertebral size to calculate apparent-level mechanical properties including Young's modulus, toughness, and ultimate stress.

2.7 Cortical bone analysis and 4-point bending test of femoral shaft

The right femurs of the cyclic treatment groups were dissected after euthanasia. A 1.2-mm region of femur midshaft was scanned by μCT (μCT 35, Scanco Medical AG, Brüttisellen, Switzerland) at 6 μm image voxel size. Bone voxels were segmented from the bone marrow and background using Gaussian filtering (sigma=1.2 and support=2.0) and a global threshold corresponding to 628.5 mgHA/cm^3. Greyscale images were then filtered (Gaussian filter, sigma=1.2, support=2), and thresholded by application of a global threshold corresponding to mgHA/cm^3. Standard cortical parameters including cortical thickness (Ct.Th), cortical porosity (Ct.Po), cortical tissue mineral density (Ct.TMD), polar moment of inertia (pMOI), periosteal perimeter (Ct.Pe.Pm), and endosteal perimeter (Ct.En.Pm) were evaluated for a 0.3 mm thick region in the center of the midshaft. A destructive 4-point bending test was then performed at the midshaft region with a displacement rate of 1.8 mm/min with the outer supports 26.6 mm apart and the inner supports 8.8 mm apart (Instron 5542, Norwood, MA). The load-displacement curve generated from mechanical testing was used to calculate stiffness, peak load, Young's modulus, energy to failure, and post-yield energy to failure [20].

2.8 Statistical Analysis

All statistical analyses were performed using NCSS 7.1.14 (NCSS, LLC, Kaysville, UT). Results were presented as boxplots with median and interquartile range (IQR; 25th to 75th percentile), and whiskers indicating maximum and minimum values. For longitudinal μCT image-based measurements, a two-way, repeated measures ANOVA was used to compare treatment groups over time. All comparisons were adjusted for baseline measures. In the presence of statistically significant main effects of time, treatment, and treatment*time interactions, *post-hoc* comparisons of between-group differences at each time point and within-group differences between different time points were made using a Bonferroni correction. For all cross-sectional group comparisons, a one-way ANOVA with a Tukey HSD *post hoc* test was performed to determine the treatment effects among groups. For all analyses, a two-tailed $p<0.05$ was considered to indicate statistical significance.

3. Results:

3.1 Sustained treatment benefits of PTH in intact rats upon 9-week discontinuation

3-week PTH treatment in intact rats caused 29% and 33% increase in tibial BV/TV and Tb.Th, and 31% and 51% decrease in Conn.D and SMI, respectively (Figure 1C–F). On the other hand, intact rats in the VEH group showed no changes in BV/TV, Tb.Th, Tb.Sp, or SMI, but an 8% decrease in Tb.N after 3 week saline treatment. BV/TV and Tb.Th were 34% and 26% greater, respectively, and SMI was 54% lower in the PTH- *vs.* VEH-treated intact rats at week 3 (Figure 1C–H).

There were sustained treatment benefits in BV/TV, Tb.Th, Tb.Sp, and Conn.D in intact animals upon 9 weeks of discontinuation of PTH, while Tb.N decreased by 5% (Figure 1C–F). By the end of week 12, BV/TV and Tb.Th were 38% and 21% greater, and SMI was 40% lower in the PTH- *vs.* VEH-treated intact rats (Figure 1C–F).

3.2 Early withdrawal from PTH is associated with an extended anabolic period in OVX rats, but not in intact rats

Before the treatment started, 4-week osteopenia development in OVX rats caused 50%, 33% and 65% decrease in tibial BV/TV, Tb.N, and Conn.D, respectively, and an increase of 146% in SMI (Figure 2C–F). Compared to week 0, 3-week VEH treatment was associated with 32% and 59% decreases in Tb.N and Conn.D, and a 71% increase in Tb.Sp, respectively. In contrast, 3-week PTH treatment effectively slowed down and partially reversed the bone loss, causing a 30% and 39% increase in BV/TV and Tb.Th, respectively and no changes in SMI, Tb.Sp, or Conn.D (Figure 2C–F). As a result, BV/TV, Tb.Th and Tb.N were 98%, 28% and 25% greater, respectively, and SMI was 30% lower in the PTH- *vs.* VEH-treated OVX rats at week 3.

Surprisingly, 1 week after discontinuation of PTH (week 4), BV/TV, Tb.Th, and SMI continued to show trends of improvement, resulting in 7% and 8% increase in BV/TV and Tb.Th, respectively, and a 8% decrease in SMI. This 1-week anabolic period upon PTH discontinuation was further confirmed on histology sections. One week after PTH discontinuation, we still observed continuous mineral apposition on the active bone forming surfaces, which were identified as the bone tissue beyond the last calcein green label injected right before the discontinuation of PTH treatment (Figure 2I). The continuous mineral apposition was found on 68% of all active bone formation surface, with an average MS/BS of 26.9%, MAR of 1.47 μm/day, and BFR/BS of 0.39 μm/day (Table 1).

Intriguingly, this extended anabolic effect upon 1-week withdrawal from PTH was only observed in OVX rats, but not in intact rats (Supplemental Figure 1B–G).

3.3 Diminished treatment benefits of PTH in OVX rats upon 9-week discontinuation

Following the 1-week extended anabolic period, a rapid decline in BV/TV occurred from the second week (week 5) upon withdrawal from PTH in OVX rats (Figure 2C). As a result, treatment benefit in BV/TV and SMI diminished and Tb.N became 23% lower as compared to week 0. 9 weeks after discontinuation of PTH, the treatment benefits in trabecular

bone were completely lost, with no difference between the PTH and VEH groups in any trabecular bone microstructure parameters (Figure 2C–F).

3.4 Acute bone cellular responses to PTH discontinuation in OVX rats but not in intact rats

3-week PTH treatment in OVX rats resulted in 117% and 107% greater N.Ob/BS and Ob.S/BS, respectively, than those treated by VEH (P3 *vs.* V3). In contrast, N.Oc/BS, Oc.S/BS and Adi.N/Ma.Ar were 55%, 52% and 69% lower in the P3 *vs.* V3 group in OVX rats, respectively (Figure 3). After 1-week withdrawal from PTH, N.Ob/BS and Ob.S/BS both decreased by 38% (P3V1 *vs* P3), respectively, but remained 36% and 30% greater than the VEH group (P3V1 *vs.* V3, Figure 3). In contrast, no change was found in N.Oc/BS and Adi.N/Ma.Ar 1 week after discontinuation of PTH (P3V1 *vs.* P3). 2-week after discontinuation of PTH, there was no remaining difference in N.Ob/BS, Ob.S/BS, N.Oc/BS and Oc.S/BS from the VEH group (P3V2 *vs.* V3) while Adi.N/Ma.Ar was still 29% lower than the VEH group (P3V2 vs. V3, Figure 3). No statistical difference was detected in serum TRAP levels among groups although the comparisons showed a similar pattern as those of N.Oc/BS and Oc.S/BS.

The responses of intact rats to the PTH treatment were similar to those of OVX rats, as demonstrated by 108% and 116% greater N.Ob/BS and Ob.S/BS, as well as 71% and 71% lower N.Oc/BS and Oc.S/BS in the PTH *vs.* VEH group, respectively (P3 *vs.* V3, Supplemental Figure 2). However, in contrast to rapid responses in bone cells to PTH discontinuation in OVX rats, in intact rats, there was no difference in any of osteoblast and osteoclast parameters between PTH-treated group and groups of 1- or 2-week after PTH discontinuation (P3 *vs.* P3V1, or P3 *vs.* P3V2, Supplemental Figure 2).

3.5 Cyclic treatment regimen alleviates PTH discontinuation-induced bone loss and extended treatment duration in OVX rats

Without therapeutic intervention, significant bone loss and trabecular bone microarchitecture deterioration occurred in the proximal tibia of the VEH-treated OVX rats over 18 weeks, resulting in 61%, 58% and 87% decreases in BV/TV, Tb.N and Conn.D, and 25% and 147% increase in Tb.Th and Tb.Sp, respectively (Figure 4C–H). In the PTH-VEH group, 9-week PTH treatment led to 99% and 92% increase in BV/TV and Tb.Th, and 18% and 56% decrease in Tb.N and SMI, respectively. After 9-week discontinuation of PTH, BV/TV and Tb.Th underwent dramatic reductions of 305% and 151% while Tb.Sp and SMI underwent substantial increases of 54% and 116%, respectively. By the end of week 18, treatment benefit of PTH was completely lost, as reflected by no difference between the PTH-VEH and VEH groups in any trabecular bone microarchitecture parameters (Figure 4C–H). In contrast, in the Cyclic PTH group, the first cycle of 3-week PTH on and 3-week off prevented reduction in BV/TV and led to a 55% increase in Tb.Th and a 24% decrease in SMI. BV/TV and SMI stabilized, and Tb.Th continued to increase during the 2nd and 3rd cycles. At week 18, BV/TV in the Cyclic PTH group was 45% and 65% greater than those of PTH-VEH and VEH group while Tb.Th was 27% and 23% greater in the Cyclic PTH group *vs.* PTH-VEH and VEH group, respectively (Figure 4C–H). However, compared to the efficacy of 9-week PTH treatment (week 9 of PTH-VEH group), 18-week cyclic

treatment (9 week total PTH) resulted in less improvement in BV/TV, Tb.N, Tb.Th, Conn.D, and SMI (Figure 4I–N).

By the end of week 18, there was no difference in any trabecular bone microarchitecture parameters or mechanical properties of the lumbar vertebra L2 between the VEH and PTH-VEH groups (Figure 5). In contrast, BV/TV of the Cyclic PTH group was 38% greater than that of the VEH group and Tb.Th was 26% and 16% greater than that of the VEH and PTH-VEH groups, respectively (Figure 5). The Cyclic PTH group also achieved better mechanical properties of L2 than the VEH group both at the whole bone level (37% and 65% greater peak load and energy to failure, respectively) and at the apparent level (84% and 53% greater toughness and ultimate stress, respectively) which were calculated by normalizing whole-bone mechanics by vertebral size (Figure 5).

Significant treatment effects were found in femur midshaft in both PTH-VEH and Cyclic PTH groups at the end of week 18 (Figure 6). pMOI and Ct.Pe.Pm in the PTH-VEH group were 28% and 6% greater than those in the VEH group, respectively, while Ct.Th in the Cyclic PTH group was 10% greater than that in the VEH group. At the whole bone level, the PTH-VEH treatment resulted in 14% and 22% greater stiffness and peak load than the VEH treatment whereas the Cyclic PTH group resulted in 25% and 43% greater peak load and total energy to failure when compared to the VEH group (Figure 6). There was no difference in any structure or mechanical properties of the femur midshaft between the PTH-VEH and the Cyclic PTH groups (Figure 6).

There were no differences between groups in animal body weight at baseline (VEH: 359±36 g, PTH-VEH: 366±12 g, and Cyclic PTH: 352±29 g) or at the end of treatments (VEH: 403±41 g, PTH-VEH: 422±18 g, and Cyclic PTH: 423±42 g). However, percent of weight gain over the 18-week treatment duration differed between groups (VEH: 12±2%, PTH-VEH: 15±3%, and Cyclic PTH 20±8%), where percent of weight gain in the Cyclic PTH group was 64% greater than that of the VEH group.

4. Discussion:

This study investigated the immediate responses in bone microstructure and bone cell activities to PTH treatment withdrawal and the associated long-term consequences. Unexpectedly, intact female and estrogen-deficient female rats had distinct responses to the discontinuation of PTH treatment. Significant tibial bone loss and bone microarchitecture deterioration occurred in estrogen-deficient rats, with the treatment benefits of PTH completely diminished 9 weeks after discontinuation. In contrast, no adverse effect was observed in intact rats, with sustained treatment benefit 9 weeks after discontinuation. Intriguingly, we discovered an extended anabolic period of bone gain upon first week withdrawal from PTH in estrogen-deficient rats. However, the extended anabolic period was not observed in intact rats upon withdrawal from PTH. Furthermore, we demonstrated that a cyclic PTH treatment regimen can efficiently leverage the extended anabolic period upon early withdrawal to alleviate withdrawal-induced bone loss and extend the PTH treatment duration in estrogen-deficient rats.

To our knowledge, this is the first study that investigated the skeletal response to discontinuation of PTH treatment in intact, adult female rats. Intermittent administration of PTH is approved for treatment of osteoporosis in postmenopausal women, hypogonadal men who are at high risk of fractures, and those with osteoporosis induced by use of glucocorticoid. In addition, it is of great clinical interest how premenopausal women with high risk of fractures respond to PTH treatment and its discontinuation. Several clinical studies have demonstrated the efficacy of PTH on preventing bone loss or improving bone mass in premenopausal women with various health conditions [21, 22] or idiopathic osteoporosis [23]. However, few data are available on skeletal changes of premenopausal women after cessation of PTH treatment [10, 24]. In a study of 38 young women with endometriosis who had been treated with a gonadotropin-releasing hormone (GnRH) analog plus PTH for 6–12 months, it was reported that BMD increased 1 year after both therapies were stopped, suggesting a persistent beneficial effect of PTH in women who regain cyclic menstrual function [24]. In a more recent study of 15 premenopausal women with idiopathic osteoporosis and normal gonadal function, it was documented that, by 2 years after discontinuation of PTH treatment BMD at the spine declined 4.8%. Moreover, this study also reported that subjects who sustained significant vertebral bone loss (>3%) after the cessation of PTH treatment were significantly older and had higher trabecular bone remodeling rate at baseline and completion of PTH treatment [10]. Our current study found sustained treatment benefit in bone mass and bone microarchitecture in female intact rats after 9-week discontinuation of PTH treatment. This is in contrast to the bone loss reported in pre-pubertal male rats [25] or estrogen-deficient rats [26–31], suggesting that skeletal responses to PTH discontinuation are influenced by estrogen status. Further investigations are required to gain more insight into the mechanisms behind the interactive effect of PTH discontinuation and estrogen status on the skeletal health.

Previous studies of ovariectomized rats have mainly focused on the long-term consequences of PTH discontinuation [26–28, 30]. Consistent with previous findings, our study demonstrated that the treatment benefit of PTH in bone mass and bone microarchitecture diminished 9 weeks after discontinuing treatment in estrogen-deficient rats. Intriguingly, unlike intact rats, trabecular bone initially continued to show trends of improvement up to 1 week after withdrawal from PTH, as demonstrated by both *in vivo* μCT and dynamic bone histomorphometry measurements. Before the cessation of PTH treatment, PTH-treated rats had lower number of osteoclasts and adipocytes and substantially increased number of osteoblasts. During the first week after treatment withdrawal, osteoclast and adipocyte numbers continued to be suppressed. In the meanwhile, the number of osteoblasts started to decline, but remained at a higher level than in the vehicle-treated rats. Continuous increase in overall bone volume fraction and newly deposited bone mineral during the first week after cessation of PTH treatment suggested that there is an extended anabolic effect upon the first week withdrawal from PTH treatment in estrogen-deficient rats. This extended anabolic period ended by the second week after withdrawal from PTH treatment, as indicated by marked increase in number of osteoclasts and adipocyte and reduction in number of osteoblasts to the levels of vehicle-treated rats. As a result, bone mass and bone microarchitecture rapidly deteriorated starting 2 weeks after discontinuation of PTH treatment.

To leverage the extended anabolic period, a cyclic treatment regimen with repeated cycles of on and off daily injection of PTH was employed. The intention was to prolong this bone-forming period to minimize the bone loss during the off-PTH cycle and extend treatment duration. The *in vivo* μCT results showed that a cyclic treatment regimen with 3 repeated cycles of on and off daily PTH injection was sufficient for maintaining trabecular bone mass and microarchitecture to prevent deterioration due to estrogen deficiency. Moreover, thickness of trabeculae was significantly improved at both the tibia and lumbar vertebra. Additionally, the cyclic treatment regimen led to a marked increase in the mechanical properties of vertebral and femoral bone as compared to the vehicle-treated rats.

The concept of administering PTH cyclically was first developed and tested by Cosman *et al.*, which was based on the observation of a rapid increase in bone formation markers before a delayed rise of bone resorption markers upon initiating PTH treatment during the first 1–6 months and a developing resistance to PTH during the second year in human patients [32–34]. It was demonstrated that the same cumulative dose of PTH given cyclically for 4 years led to comparable increase of BMD as standard daily PTH administration over 2 years [33]. In the current study, we further hypothesize that the extended anabolic effect upon early discontinuation of PTH would help dampen the loss during the off-PTH cycle. However, compared to the efficacy of standard 9-week PTH treatment in rats, cyclic treatment regimens consisting of three 3-week PTH cycles, each followed by 3-week off (9 week total PTH) resulted in a lower peak improvement in bone volume and bone microarchitecture. A limitation of the cyclic treatment regimen used in the current study is that the off treatment period of 3 weeks exceeded the duration of the extended anabolic period upon early withdrawal. As suggested by histomorphometry results, osteoclast number and surface started to increase following 2-week discontinuation of PTH, thus resulting in PTH withdrawal-induced bone loss. Indeed, considering the difference between human and rat's life span, a 3-week duration in rats corresponds to ~18 months in humans [35], which far exceeds the recommended cyclic treatment duration of 3 months in humans. Therefore, further research is required to test whether a shorter duration of cyclic treatment in rats may better model the therapeutic potential of the cyclic treatment regimen applied in a clinical setting. Nevertheless, current study demonstrated the concept of the cyclic treatment regimen in a rat model, which leverages the extended anabolic period upon early withdrawal of PTH to enhance treatment efficacy and extend treatment duration.

A major limitation of the current study is the discrepancy between human and rats in their responses of osteoclast activities to PTH. Intermittent PTH administration led to increases in both bone formation and bone resorption markers in postmenopausal women. However, our results in both intact and estrogen deficient rats indicated increased number and surface of osteoblasts and suppressed number and surface of osteoclasts after 3-week PTH treatment. Similar observations of either reduced or unchanged osteoclast numbers/surface in PTH-treated rats were also reported in previous studies of rat models [26–28, 36–38]. Still, the reason causing the discrepancy between the clinical findings and rat model is not completely understood. There are, however, several possible explanations. In one of our recent studies, by using multiple fluorochrome labeling to track bone formation activated at different timing during a 3-week period, we found that remodeling-based bone formation, *i.e.*, new bone formation elicited on resorbed bone surface by osteoclasts, was 4.9 times greater in

PTH-treated *vs.* VEH-treated rats. Strikingly, 66% of these osteoclast resorption-initiated bone formation sites occurred within 24–48 hours of initiation of PTH treatment and 98% within the first week of treatment [39]. The lack of new osteoclast resorption-initiated bone formation sites after the first week of PTH treatment suggested that osteoclast activities quickly went up in response to PTH, but then diminished after the first week of treatment. It has been established that PTH indirectly regulates osteoclastogenesis to enhance bone resorption, by modulating the expression of the receptor activator of nuclear factor-kappa B ligand (RANKL) and its soluble decoy receptor osteoprotegerin (OPG) in osteoblasts and osteocytes [40–43]. We speculate that the rapidly increased RANKL/OPG ratio in response to PTH exhausted the progenitor pool of osteoclasts within a week of treatment under the current treatment dose in rats. Therefore, in the current study, osteoclast number and surface significantly reduced after 3-week PTH treatment. Indeed, in a study where rats were treated with PTH for near-lifetime (2-years), prominent osteoblasts but near absence of osteoclasts were found in rat femora, tibia and vertebra [37]. Another discrepancy between rats and humans is PTH treatment dose. The typic range of PTH dose applied to rats (20–100 μg/kg/day, 40 μg/kg/day in the current study) is 5–25 times higher than the equivalent human dose [44] recommended by the FDA. This discrepancy could cause different dynamic responses of osteoclast resorption. Further research is required to establish the PTH dosage and treatment duration in rodents to achieve skeletal responses that more accurately reflect clinical observations in human patients.

Despite these limitations, this study has several notable strengths. The current study is the first to use an advanced *in vivo* μCT imaging and image analysis techniques to longitudinally track changes taking place as a result of discontinuation of PTH administration in rats. The high temporal and spatial resolution of the *in vivo* μCT imaging technique allowed sensitive detection of subtle changes in bone microarchitecture and enabled the discovery of an extended anabolic period upon discontinuation of PTH treatment in estrogen deficient rats. This is also the first study which compared skeletal responses to cessation of PTH treatment between intact and estrogen-deficient rats, which may provide important insight in therapeutic strategies of follow-up treatment after PTH treatment in young women. Lastly, this study explored the cyclic treatment regimen as an option to extend treatment duration under the same cumulative treatment dosage. While the extended anabolic period achieved additional bone gain during the early time of an off-PTH cycle, it failed to fully prevent PTH discontinuation-induced bone loss by the end of an off cycle. Clinically, it has been recommended that anti-resorptive treatment should be applied upon discontinuation of PTH to prevent bone loss. Therefore, to sustain PTH treatment efficacy while extending treatment duration, further studies should be undertaken to test the cyclic treatment regimen by alternating PTH and anti-resorptive treatment.

In summary, this study demonstrated distinct skeletal responses to cessation of PTH treatment between intact and estrogen deficient female rats, suggesting that different follow-up treatment strategies may be considered for pre- and post-menopausal women. An extended anabolic period upon early withdrawal from PTH treatment offered a new mechanism in support of cyclic treatment regimen with repeated cycles of on and off PTH treatment, which alleviated PTH withdrawal-induced bone loss, improved bone mass, bone microarchitecture, and whole-bone mechanical properties, and extended treatment duration.

Supplementary Material

Refer to Web version on PubMed Central for supplementary material.

Acknowledgement

Research reported in this publication was supported by the Penn Center for Musculoskeletal Diseases (PCMD) NIH/NIAMS P30-AR069619, NIH/NIAMS K01-AR066743 (to XSL), and National Science Foundation (NSF) Award #1661858 (to XSL).

References

1. NIH Consensus Development Panel on Osteoporosis Prevention, Diagnosis, and Therapy. Osteoporosis prevention, diagnosis, and therapy. JAMA. 2001;285(6):785–795. [PubMed: 11176917]
2. Watts NB and Bilezikian JP, Advances in target-specific therapy for osteoporosis. J Clin Endocrinol Metab, 2014. 99(4): p. 1149–51. [PubMed: 24446660]
3. Jilka RL, Molecular and cellular mechanisms of the anabolic effect of intermittent PTH. Bone, 2007. 40(6): p. 1434–46. [PubMed: 17517365]
4. Compston JE, Skeletal actions of intermittent parathyroid hormone: effects on bone remodelling and structure. Bone, 2007. 40(6): p. 1447–52. [PubMed: 17045858]
5. Qin L, Raggatt LJ, and Partridge NC, Parathyroid hormone: a double-edged sword for bone metabolism. Trends Endocrinol Metab, 2004. 15(2): p. 60–5. [PubMed: 15036251]
6. Vahle JL, Long GG, Sandusky G, Westmore M, Ma YL, and Sato M, Bone neoplasms in F344 rats given teriparatide [rhPTH(1–34)] are dependent on duration of treatment and dose. Toxicol Pathol, 2004. 32(4): p. 426–38. [PubMed: 15204966]
7. Vahle JL, Sato M, Long GG, Young JK, Francis PC, Engelhardt JA, Westmore MS, Linda Y, and Nold JB, Skeletal changes in rats given daily subcutaneous injections of recombinant human parathyroid hormone (1–34) for 2 years and relevance to human safety. Toxicol Pathol, 2002. 30(3): p. 312–21. [PubMed: 12051548]
8. Jolette J, Wilker CE, Smith SY, Doyle N, Hardisty JF, Metcalfe AJ, Marriott TB, Fox J, and Wells DS, Defining a noncarcinogenic dose of recombinant human parathyroid hormone 1–84 in a 2-year study in Fischer 344 rats. Toxicol Pathol, 2006. 34(7): p. 929–40. [PubMed: 17178693]
9. Black DM, Bilezikian JP, Ensrud KE, Greenspan SL, Palermo L, Hue T, Lang TF, McGowan JA, Rosen CJ, and Pa THSI, One year of alendronate after one year of parathyroid hormone (1–84) for osteoporosis. N Engl J Med, 2005. 353(6): p. 555–65. [PubMed: 16093464]
10. Cohen A, Kamanda-Kosseh M, Recker RR, Lappe JM, Dempster DW, Zhou H, Cremers S, Bucovsky M, Stubby J, and Shane E, Bone Density After Teriparatide Discontinuation in Premenopausal Idiopathic Osteoporosis. J Clin Endocrinol Metab, 2015. 100(11): p. 4208–14. [PubMed: 26358172]
11. Leder BZ, Neer RM, Wyland JJ, Lee HW, Burnett-Bowie SM, and Finkelstein JS, Effects of teriparatide treatment and discontinuation in postmenopausal women and eugonadal men with osteoporosis. J Clin Endocrinol Metab, 2009. 94(8): p. 2915–21. [PubMed: 19435827]
12. Altman AR, Tseng WJ, de Bakker CM, Huh BK, Chandra A, Qin L, and Liu XS, A closer look at the immediate trabecula response to combined parathyroid hormone and alendronate treatment. Bone, 2014. 61C: p. 149–157.
13. Bach-Gansmo FL, Irvine SC, Bruel A, Thomsen JS, and Birkedal H, Calcified cartilage islands in rat cortical bone. Calcif Tissue Int, 2013. 92(4): p. 330–8. [PubMed: 23274728]
14. Lan S, Luo S, Huh BK, Chandra A, Altman AR, Qin L, and Liu XS, 3D image registration is critical to ensure accurate detection of longitudinal changes in trabecular bone density, microstructure, and stiffness measurements in rat tibiae by in vivo micro computed tomography (μCT). Bone, 2013. 56(1): p. 83–90. [PubMed: 23727434]
15. Altman AR, Jeong Y, Tseng WJ, De Bakker CM, Qin L, Han L, Kim DG, and Liu XS Intermittent PTH alleviates abnormalities of bone tissue heterogeneity associated with prolonged

bisphosphonate treatment by inducing substantial new bone formation. in Annual Meeting of American Society of Bone and Mienral Research. 2015.

16. Bouxsein ML, Boyd SK, Christiansen BA, Guldberg RE, Jepsen KJ, and Muller R, Guidelines for assessment of bone microstructure in rodents using micro-computed tomography. J Bone Miner Res, 2010. 25(7): p. 1468–86. [PubMed: 20533309]
17. Dempster DW, Compston JE, Drezner MK, Glorieux FH, Kanis JA, Malluche H, Meunier PJ, Ott SM, Recker RR, and Parfitt AM, Standardized nomenclature, symbols, and units for bone histomorphometry: a 2012 update of the report of the ASBMR Histomorphometry Nomenclature Committee. J Bone Miner Res, 2013. 28(1): p. 2–17. [PubMed: 23197339]
18. Parfitt AM, Drezner MK, Glorieux FH, Kanis JA, Malluche H, Meunier PJ, Ott SM, and Recker RR, Bone histomorphometry: standardization of nomenclature, symbols, and units. Report of the ASBMR Histomorphometry Nomenclature Committee. J Bone Miner Res, 1987. 2(6): p. 595–610. [PubMed: 3455637]
19. Pendleton MM, Sadoughi S, Li A, O'Connell GD, Alwood JS, and Keaveny TM, High-precision method for cyclic loading of small-animal vertebrae to assess bone quality. Bone Rep, 2018. 9: p. 165–172. [PubMed: 30417036]
20. Schriefer JL, Robling AG, Warden SJ, Fournier AJ, Mason JJ, and Turner CH, A comparison of mechanical properties derived from multiple skeletal sites in mice. J Biomech, 2005. 38(3): p. 467–75. [PubMed: 15652544]
21. Fazeli PK, Wang IS, Miller KK, Herzog DB, Misra M, Lee H, Finkelstein JS, Bouxsein ML, and Klibanski A, Teriparatide increases bone formation and bone mineral density in adult women with anorexia nervosa. J Clin Endocrinol Metab, 2014. 99(4): p. 1322–9. [PubMed: 24456286]
22. Hong N, Kim JE, Lee SJ, Kim SH, and Rhee Y, Changes in bone mineral density and bone turnover markers during treatment with teriparatide in pregnancy- and lactation-associated osteoporosis. Clin Endocrinol (Oxf), 2018. 88(5): p. 652–658. [PubMed: 29389010]
23. Cohen A, Stein EM, Recker RR, Lappe JM, Dempster DW, Zhou H, Cremers S, McMahon DJ, Nickolas TL, Muller R, Zwahlen A, Young P, Stubby J, and Shane E, Teriparatide for idiopathic osteoporosis in premenopausal women: a pilot study. J Clin Endocrinol Metab, 2013. 98(5): p. 1971–81. [PubMed: 23543660]
24. Finkelstein JS and Arnold AL, Increases in bone mineral density after discontinuation of daily human parathyroid hormone and gonadotropin-releasing hormone analog administration in women with endometriosis. J Clin Endocrinol Metab, 1999. 84(4): p. 1214–9. [PubMed: 10199756]
25. Gunness-Hey M and Hock JM, Loss of the anabolic effect of parathyroid hormone on bone after discontinuation of hormone in rats. Bone, 1989. 10(6): p. 447–52. [PubMed: 2624826]
26. Ma YL, Bryant HU, Zeng Q, Schmidt A, Jee WS, and Sato M, Raloxifene and teriparatide (hPTH 1–34) have complementary effects on the osteopenic skeleton of ovariectomized rats. J Bone Miner Metab, 2005. 23 Suppl: p. 62–8. [PubMed: 15984416]
27. Iwaniec UT, Samnegard E, Cullen DM, and Kimmel DB, Maintenance of cancellous bone in ovariectomized, human parathyroid hormone [hPTH(1–84)]-treated rats by estrogen, risedronate, or reduced hPTH. Bone, 2001. 29(4): p. 352–60. [PubMed: 11595618]
28. Takano Y, Tanizawa T, Mashiba T, Endo N, Nishida S, and Takahashi HE, Maintaining bone mass by bisphosphonate incadronate disodium (YM175) sequential treatment after discontinuation of intermittent human parathyroid hormone (1–34) administration in ovariectomized rats. J Bone Miner Res, 1996. 11(2): p. 169–77. [PubMed: 8822340]
29. Ma Y, Jee WS, Chen Y, Gasser J, Ke HZ, Li XJ, and Kimmel DB, Partial maintenance of extra cancellous bone mass by antiresorptive agents after discontinuation of human parathyroid hormone (1–38) in right hindlimb immobilized rats. J Bone Miner Res, 1995. 10(11): p. 1726–34. [PubMed: 8592950]
30. Yamamoto N, Takahashi HE, Tanizawa T, Fujimoto R, Hara T, and Tanaka S, Maintenance of bone mass by physical exercise after discontinuation of intermittent hPTH(1–34) administration. Bone Miner, 1993. 23(3): p. 333–42. [PubMed: 8148673]
31. Shahnazari M, Yao W, Wang B, Panganiban B, Ritchie RO, Hagar Y, and Lane NE, Differential maintenance of cortical and cancellous bone strength following discontinuation of bone-active agents. J Bone Miner Res, 2011. 26(3): p. 569–81. [PubMed: 20839286]

32. Cosman F, Nieves J, Zion M, Woelfert L, Luckey M, and Lindsay R, Daily and cyclic parathyroid hormone in women receiving alendronate. New England Journal of Medicine, 2005. 353(6): p. 566–575. [PubMed: 16093465]
33. Cosman F, Nieves JW, Roimisher C, Neubort S, McMahon DJ, Dempster DW, and Lindsay R, Administration of teriparatide for four years cyclically compared to two years daily in treatment Naive and alendronate treated women. Bone, 2019. 120: p. 246–253. [PubMed: 30355512]
34. Cosman F, Nieves JW, Zion M, Garrett P, Neubort S, Dempster D, and Lindsay R, Daily or Cyclical Teriparatide Treatment in Women With Osteoporosis on no Prior Therapy and Women on Alendronate. J Clin Endocrinol Metab, 2015. 100(7): p. 2769–76. [PubMed: 25961136]
35. Sengupta P, The Laboratory Rat: Relating Its Age With Human's. Int J Prev Med, 2013. 4(6): p. 624–30. [PubMed: 23930179]
36. Liu CC and Kalu DN, Human parathyroid hormone-(1–34) prevents bone loss and augments bone formation in sexually mature ovariectomized rats. J Bone Miner Res, 1990. 5(9): p. 973–82. [PubMed: 2281827]
37. Sato M, Vahle J, Schmidt A, Westmore M, Smith S, Rowley E, and Ma LY, Abnormal bone architecture and biomechanical properties with near-lifetime treatment of rats with PTH. Endocrinology, 2002. 143(9): p. 3230–42. [PubMed: 12193534]
38. Altman-Singles AR, Jeong Y, Tseng WJ, de Bakker CM, Zhao H, Lott C, Robberts J, Qin L, Han L, Kim DG, and Liu XS, Intermittent Parathyroid Hormone After Prolonged Alendronate Treatment Induces Substantial New Bone Formation and Increases Bone Tissue Heterogeneity in Ovariectomized Rats. J Bone Miner Res, 2017. 32(8): p. 1703–1715. [PubMed: 28467646]
39. Wang W, Tseng WJ, Zhao H, Azar T, Pei S, Jiang X, Dyment N, and Liu XS, Activation, development, and attenuation of modeling- and remodeling-based bone formation in adult rats. Biomaterials, 2021. 276: p. 121015. [PubMed: 34273687]
40. Lee SK and Lorenzo JA, Parathyroid hormone stimulates TRANCE and inhibits osteoprotegerin messenger ribonucleic acid expression in murine bone marrow cultures: correlation with osteoclast-like cell formation. Endocrinology, 1999. 140(8): p. 3552–61. [PubMed: 10433211]
41. O'Brien CA, Nakashima T, and Takayanagi H, Osteocyte control of osteoclastogenesis. Bone, 2013. 54(2): p. 258–63. [PubMed: 22939943]
42. Kanzawa M, Sugimoto T, Kanatani M, and Chihara K, Involvement of osteoprotegerin/osteoclastogenesis inhibitory factor in the stimulation of osteoclast formation by parathyroid hormone in mouse bone cells. Eur J Endocrinol, 2000. 142(6): p. 661–4. [PubMed: 10822231]
43. Silva BC and Bilezikian JP, Parathyroid hormone: anabolic and catabolic actions on the skeleton. Curr Opin Pharmacol, 2015. 22: p. 41–50. [PubMed: 25854704]
44. Estimating the maximum safe starting dose in initial clinical trials for therapeutics in adult healthy volunteers. US FDA, 2005. https://www.fda.gov/media/72309/download

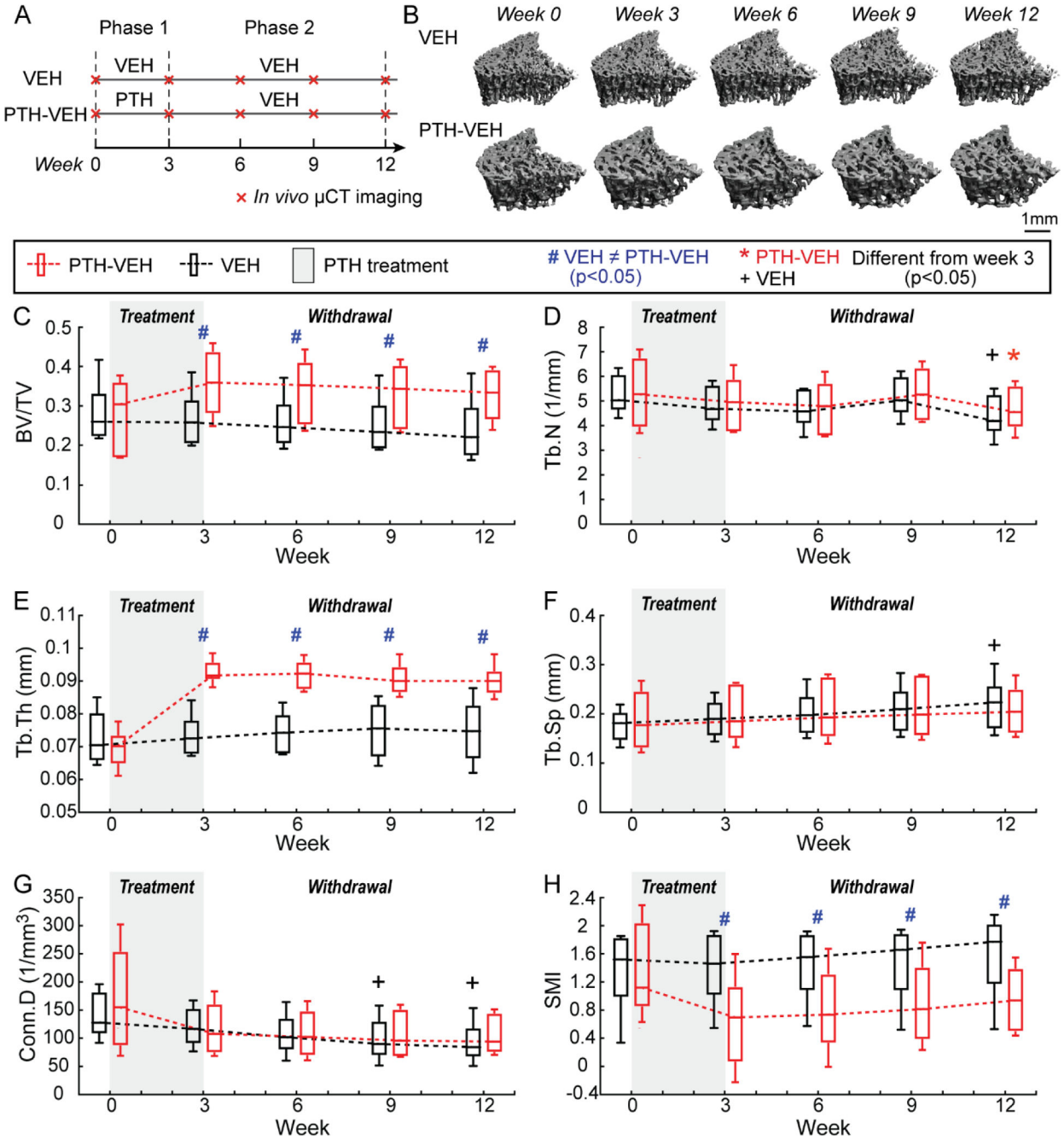

Figure 1.

Intact Animals (A) Schematics of treatment strategies, (B) Representative 3D renderings of the proximal tibia of a VEH and PTH-VEH rat at weeks 0, 3, 6, 9, 12. (C-H) Changes in tibial trabecular bone microstructure measurements in PTH-VEH and VEH groups (Mean±SD, n=6/group). # indicates a significant difference between PTH-VEH and VEH groups ($p<0.05$). + indicates a significant difference from week 3 in VEH group ($p<0.05$). * indicates a significant difference from week 3 in PTH-VEH group ($p<0.05$).

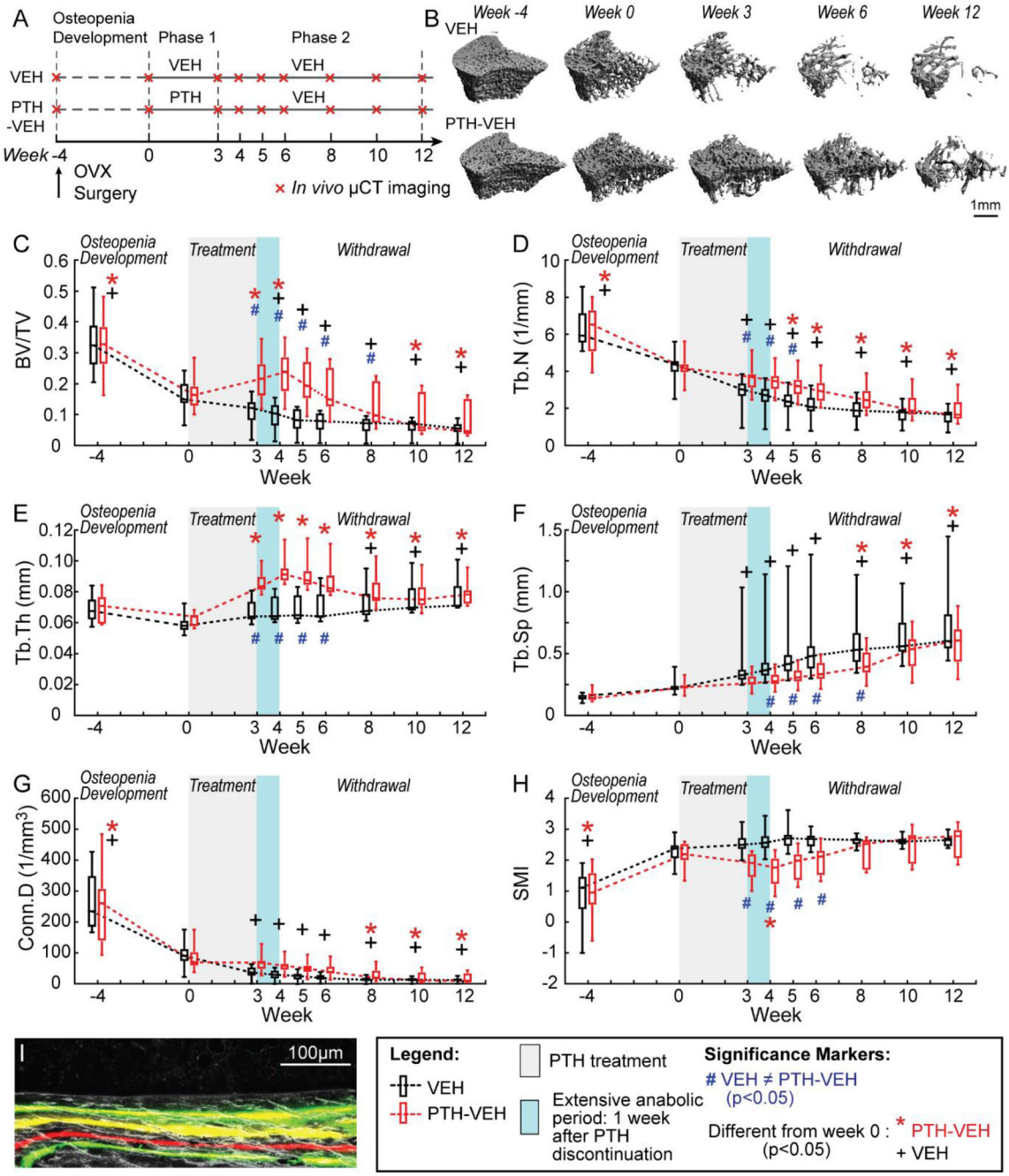

Figure 2.

Estrogen-deficient animals (A) Schematics of treatment strategies, (B) Representative 3D renderings of the proximal tibia of a VEH and PTH-VEH rat at weeks −4, 0, 3, 6, 12. (C-H) Changes in tibial trabecular bone microstructure measurements in PTH-VEH and VEH groups (Mean±SD, n=9/group). (I) Representative dynamic histomorphometry image indicating continued mineral apposition one week after PTH discontinuation. # indicates a significant difference between PTH-VEH and VEH groups ($p<0.05$). + indicates a significant difference from week 0 in VEH group ($p<0.05$). * indicates a significant difference from week 0 in PTH-VEH group ($p<0.05$).

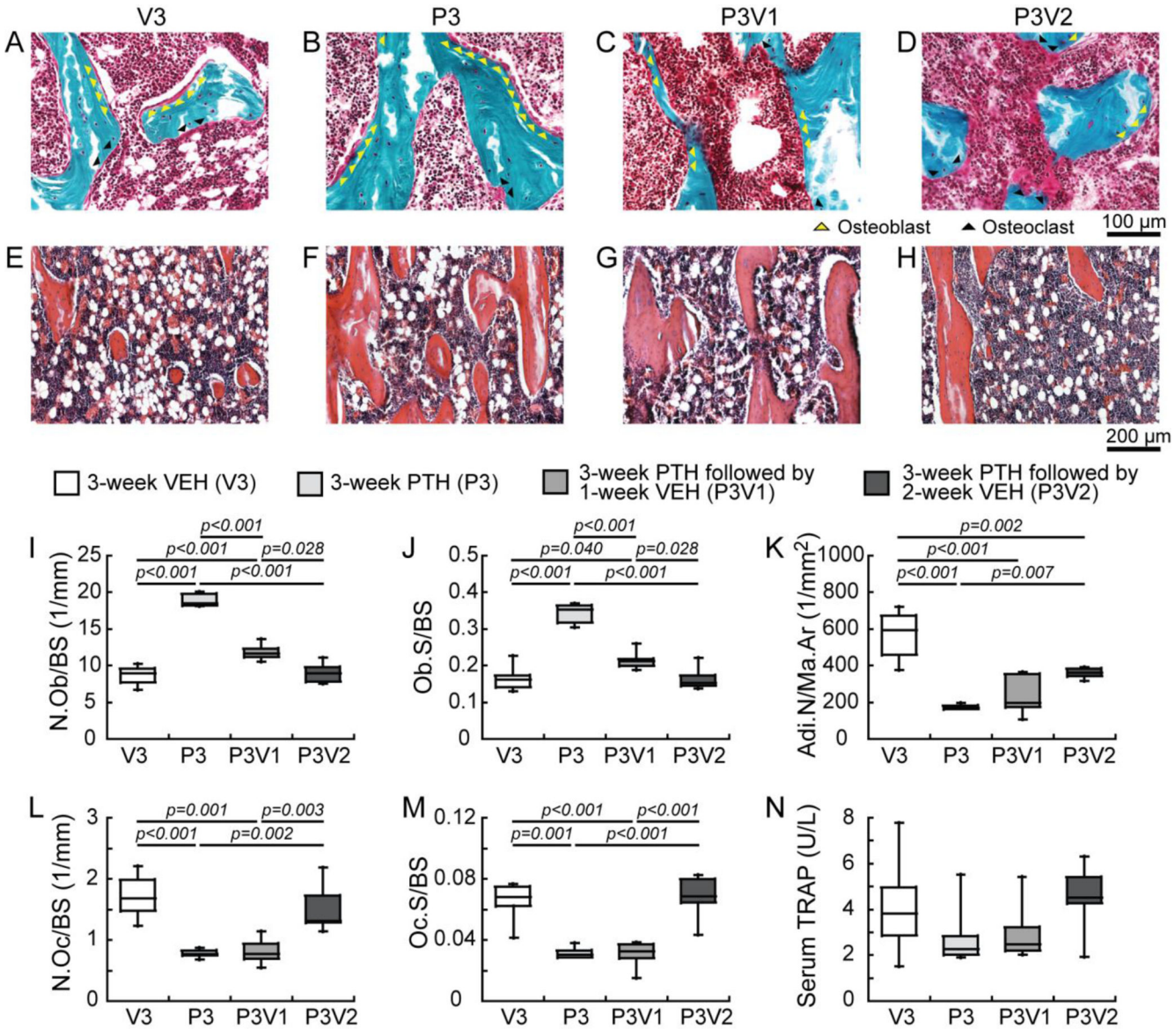

Figure 3.

Estrogen-deficient animals (A-D) Osteoblasts (yellow arrows) and osteoclasts (black arrows) are shown with Goldner's Trichrome staining of trabecular bone sections in OVX rats with (A) 3-week VEH (V3) and (B) PTH (P3) treatments, and 3-week PTH treatment followed by (C) 1 and (D) 2 weeks withdrawal (P3V1 and P3V2). Adipocytes are shown with H&E staining of trabecular bone sections in OVX rats at (E) V3, (F) P3, (G) P3V1, and (H) P3V2. Histomorphometric measurements of (I) osteoblast number (N.Ob/BS), (J) osteoblast surface (Ob.S/BS), (K) adipocyte number (Adi.N/Ma.Ar), (L) osteoclast number (N.Oc/BS), (M) osteoclast surface (Oc.S/BS), (N) ELISA analysis of serum concentration of bone resorption (TRAcP 5b) marker were measured for V3, P3, P3V1, P3V2 (n=6/group).

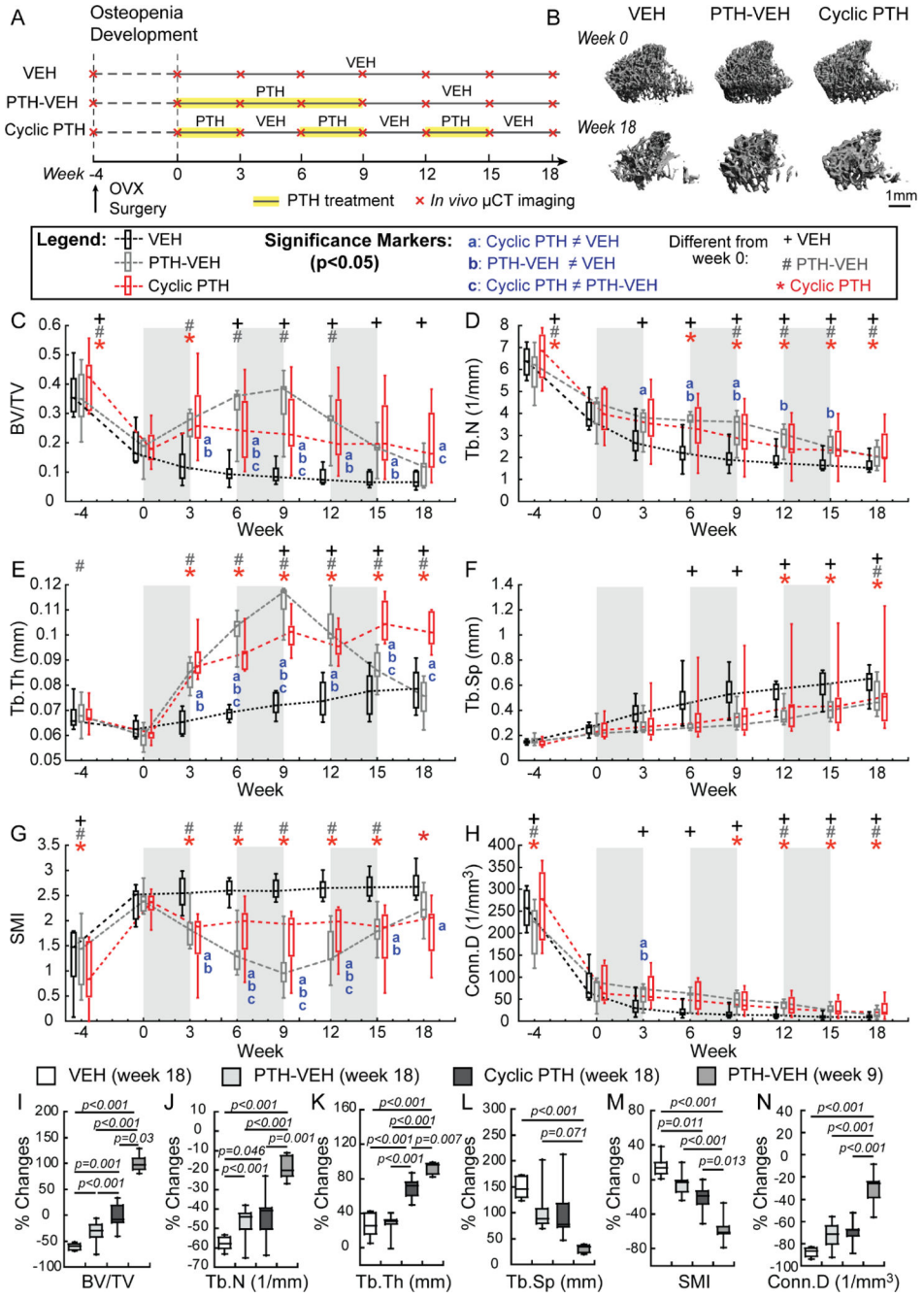

Figure 4.

Estrogen-deficient animals in cyclic treatment regimens (A) Schematics of treatment strategies, (B) Representative 3D renderings of the proximal tibia of a VEH, PTH-VEH, and Cyclic PTH rat at weeks 0 and 18. (C-H) Changes in tibial trabecular bone microstructure measurements in VEH (n=6), PTH-VEH (n=7), and Cyclic PTH (n=7) groups (Mean±SD). a indicates a significant difference between Cyclic PTH and VEH groups ($p<0.05$). b indicates a significant difference between PTH-VEH and VEH groups ($p<0.05$). c indicates a significant difference between in Cyclic PTH and PTH-VEH groups ($p<0.05$). + indicates a significant difference from week 0 in VEH group ($p<0.05$). # indicates a significant

difference from week 0 in PTH-VEH group ($p<0.05$). * indicates a significant difference from week 0 in Cyclic PTH group ($p<0.05$). (I-N) Comparisons of percent changes of tibial trabecular bone microstructure from week 0 between VEH (at week 18), PTH-VEH (at week 18), Cyclic PTH (at week 18), and PTH-VEH (at week 9).

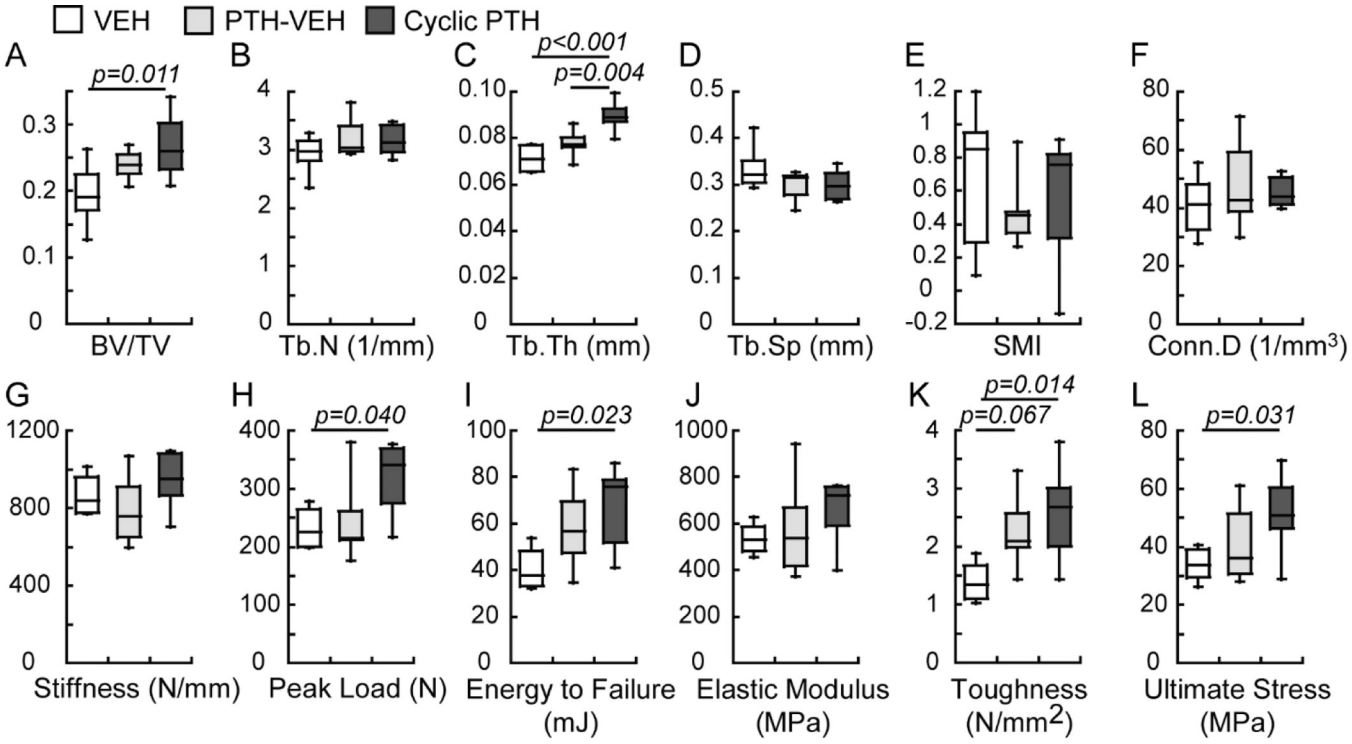

Figure 5.

Comparisons between treatment groups (n=6–7/group) in cyclic treatment regimens at the end of week 18 in trabecular bone microstructure and mechanical properties of lumbar vertebra L2.

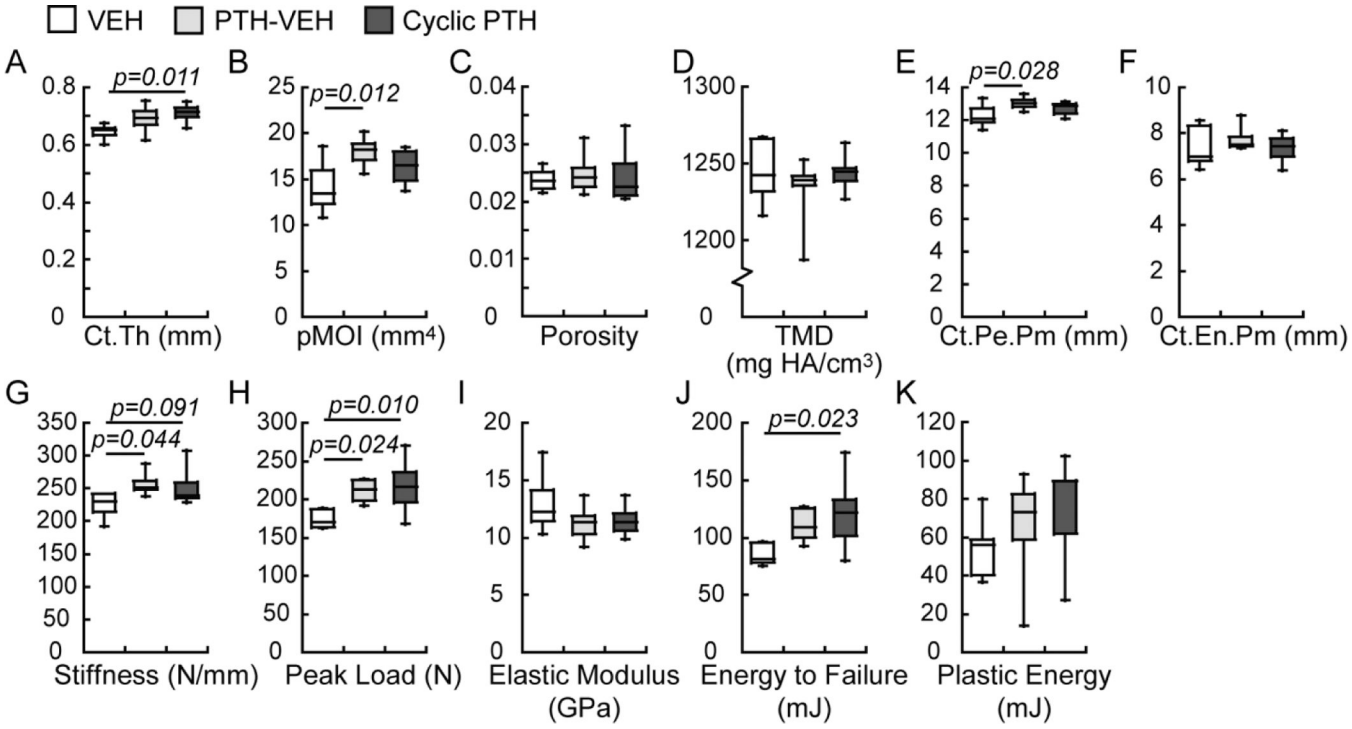

Figure 6.

Comparisons between treatment groups (n=6–7/group) in cyclic treatment regimens at the end of week 18 in cortical bone microstructure and mechanical properties of femur.

Table 1.

Dynamic histomorphometry analysis of bone formation during a 1-week anabolic period upon PTH discontinuation (n=6).

	Mean±SD	Median	Min	Max
MS/BS (%)	26.9±3.3	25.4	24.4	32.8
MAR (μm/day)	1.47±0.16	1.42	1.29	1.69
BFR/BS (μm/day)	0.39±0.04	0.38	0.34	0.45